Electronic Suppporting Information for

"Dynamics in hydrated inorganic nanotubes studied by neutron scattering: towards nanoreactors in water"

Sophie Le Caër[a], Marie-Claire Pignié[a], Quentin Berrod[b], Veronika Grzimek[c], Margarita Russina[c], Cédric Carteret[d], Antoine Thill[a], Jean-Marc Zanotti[e] and José Teixeira[d]*

[a] *NIMBE, UMR 3685 CEA, CNRS, Université Paris-Saclay, CEA Saclay 91191 Gif-sur-Yvette Cedex, France.*

[b] *CNRS-CEA-Université Grenoble Alpes SyMMES, 38000 Grenoble, France*

[c] *Helmholtz-Zentrum Berlin für Materialien und Energie, Hahn-Meitner-Platz 1, 14109 Berlin, Germany*

[d] *Université de Lorraine, CNRS, LCPME, 54000 Nancy, France*

[e] *Laboratoire Léon Brillouin, CEA-CNRS (UMR-12), CEA Saclay, Université Paris-Saclay, 91191 Gif-sur-Yvette Cedex, France.*

**email : sophie.le-caer@cea.fr*

Simulation of water sorption isotherm

Imogolite adsorb water on two distinct surfaces. Part of the water is adsorbed inside the internal pore of the nanotube whose internal surface is very hydrophilic in the case of IMO-OH and very hydrophobic in the case of IMO-CH_3. Part of the water is also adsorbed on the external surface of the nanotubes which is covered by Al-OH-Al groups for both imogolites. The curvature of the two types of tubes is however different and may change strongly the affinity for water.[1] The presence of these two surfaces make the distinction of internal and external adsorbed water a challenging task which requires the use of a model.[2,3] The theoretical modeling of the internal water adsorption is highly dependent on the water model and on the motions of the internal hydroxyl groups.[3,4] For external water, the task is very difficult due to the impact of the bundle packing and of the presence of impurities (salt). [3]

The affinity between water and the two surfaces controls the amount of adsorbed water as a function of RH. The structure of the nanotube packing plays also an important role in the external water adsorption by controlling the size distribution and shape of the pores. The total amount of water adsorbed was measured at each RH value for both imogolites (Figure 1 in the

main text). In order to estimate the proportion of internal and external water, a model of the water adsorption which takes into account the contrasted water affinity between the inside and outside surface and also the powder structure, has to be used. The model is based on the water filling of a 2D random arrangement of imogolite nanotubes. To build this random packing, a defined number of nanotubes (not overlapping) are first randomly placed on a 2D matrix. Then 2D hexagonal crystals are grown around each nanotube until a defined solid volume fraction φ is reached. φ is chosen so that the whole available space is filled by water at RH = 100%.

The water adsorption has two distinct regimes in our model. At low RH values, when less than a monolayer of water is adsorbed on average, the quantity of adsorbed water is well described by the BET equation:

$$\frac{m}{m_0} = \frac{c * \frac{p}{p_0}}{(1 - \frac{p}{p_0})(1 - \frac{p}{p_0} + c\frac{p}{p_0})}$$

with *m* the mass of adsorbed water, m_0 the mass of a monolayer, $\frac{p}{p_0}$ the ratio between equilibrium and saturation pressures (equal to the RH value, once multiplied by 100) and *c* the BET constant describing the affinity of water for the surface. In the present model, two distinct BET constants are considered; c_{in} and c_{out} for the internal and external surfaces, respectively.

At higher RH values, when more than a monolayer is adsorbed on average, the system behaves differently. The water layer starts to be continuous on the surface and an interfacial tension is then active giving rise to capillary condensation. To describe the equilibrium of the water layer as a function of RH at both internal and external surfaces, we used a method adapted from Or and Tuller.[5] In this second regime, the chemical potential (μ) of the water film is the sum of two contributions: an adsorption component *A(h)* and a capillary component *C(k)*, with *h* the water film thickness and $k = 1/r_c$ the film curvature. Taking into account van der Waals effects only, the chemical potential is expressed as:

$$\mu = \frac{A_{svl}}{6\pi\rho h^3} - 2\frac{\sigma k}{\rho}$$

with A_{svl} the Hamaker constant for solid-vapor interaction through the liquid film ($A_{svl} < 0$ for adsorption), ρ the liquid density and σ the surface tension of the liquid-vapor interface. To have a self-consistency between the low RH and high RH regime, we ensure that the same water

monolayer thickness is obtained at the common RH value. According to the BET equation, the monolayer thickness h_0 is obtained when $\frac{p}{p_0} = \frac{1}{1+\sqrt{c}}$.

So we use $A_{svl} = 6\pi\rho h_0^3 \frac{RT}{M} \ln(\frac{p}{p_0})$, with M the molecular weight of the water molecule and h_0 equal to 2.3 Å (which correponds to the thickness of a water layer).

At each RH value, the random imogolite matrix is filled with water respecting the minimum film thickness h and the minimum film curvature k as shown on Figure S1. The water percentage can then be expressed as a function of the number of pixels occupied by water and by imogolite.

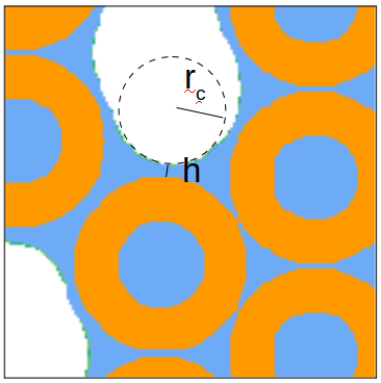

Fig. S1. *Picture of the imogolite random packing showing the rules for water filling.*

For IMO-OH, the water adsorption isotherm is well described if one consideres dense bundles of nanotubes. Between each bundle, only a few large mesopores exists. Figure S2 shows the model water adsorption in IMO-OH and the snapshots of the simulated matrix for RH = 3, 11, 43 and 74%.

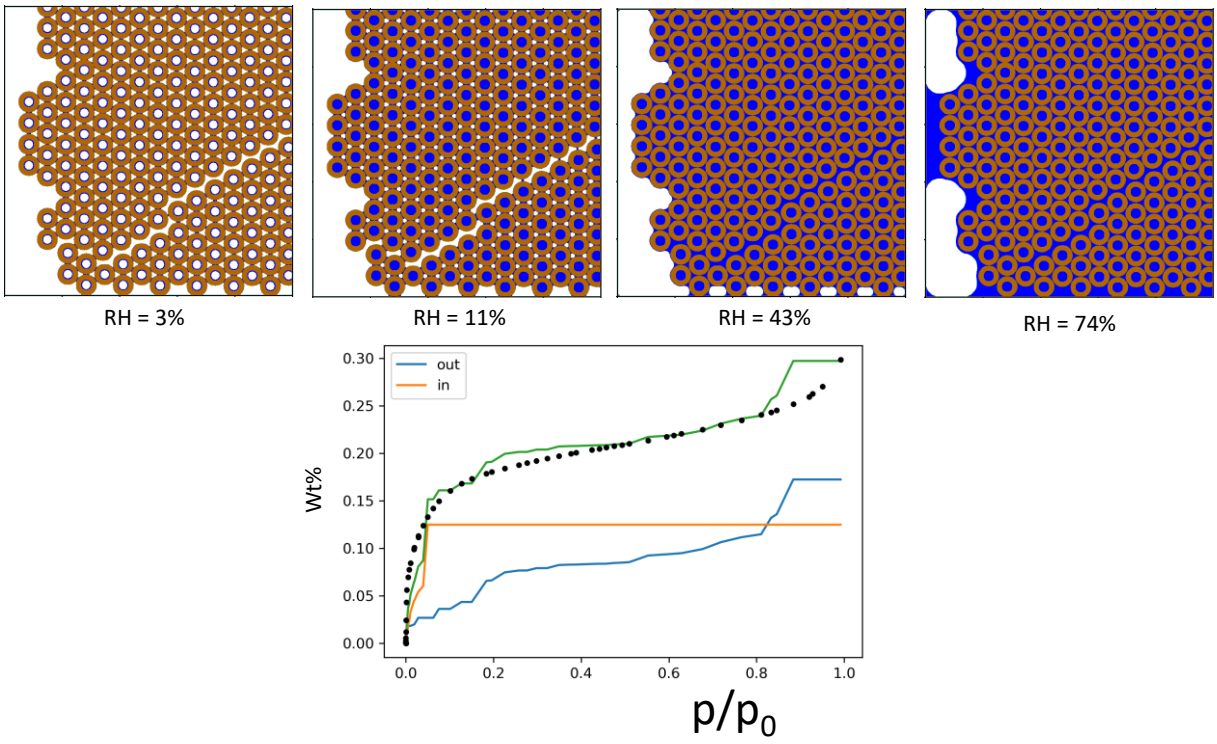

Fig. S2. *(Top) Snapshots of water filling in IMO-OH at selected RH values. (Bottom) Experimental water isotherm (points) together with the simulation (green line). The water percentage present inside or outside the tubes is displayed with an orange and blue color, respectively as a function of* p/p_0.

For IMO-CH_3, the water adsorption isotherm is very different. To reproduce the observed adsorption behavior, very small bundles with a distribution of mesopores between them have to be considered. Figure S3 shows the simulated isotherm with snapshots of the matrix at RH = 3, 11, 43 and 74%. Only external water enables is present.

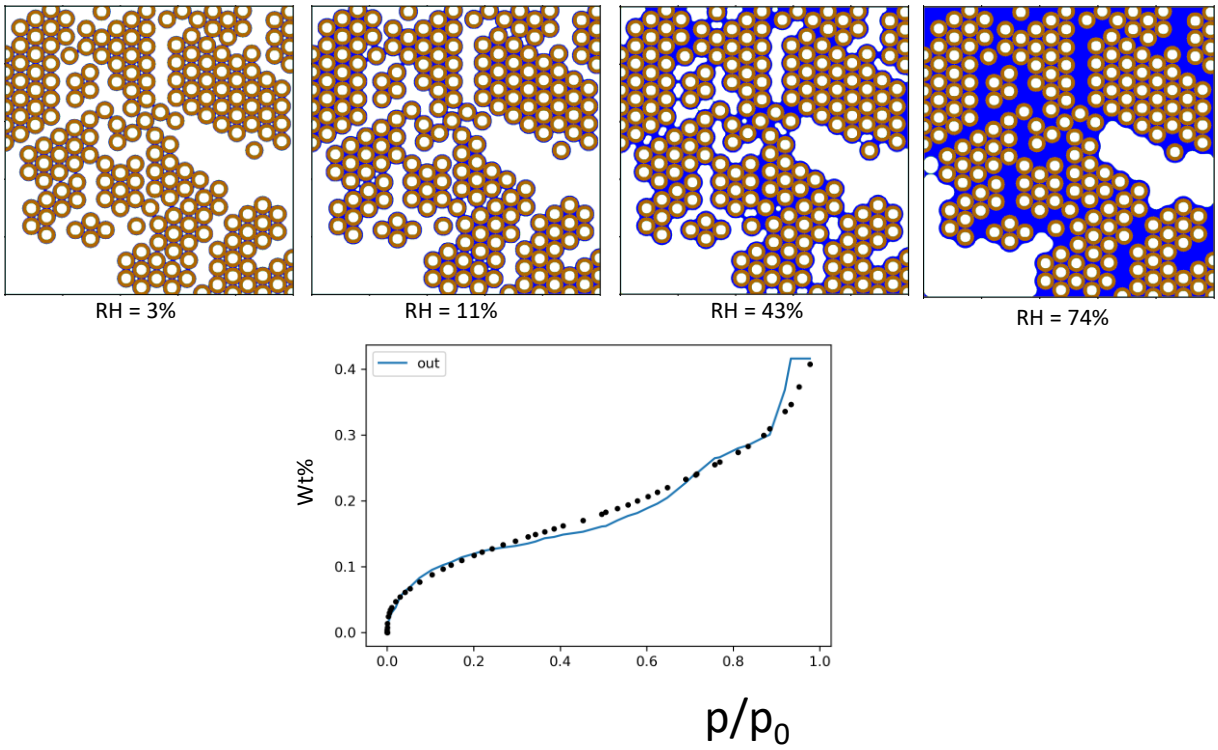

Fig. S3. *(Top) Snapshots of water filling in IMO-CH_3 at selected RH values. (Bottom) Experimental water isotherm (points) together with the simulation (blue line). The water percentage present outside the tubes is displayed as a function of p/p_0.*

TEM images of dried suspensions of imogolites

A 5 µL drop of an aqueous imogolite suspension (~80 $mg.L^{-1}$) was deposited on a copper grid covered with a carbon film (Agar Scientific). The excess liquid was blotted off with paper filter after about 10 seconds.

Transmission electron microscopy (TEM) was performed on a Philips CM12 electron microscope operated at 80 kV. Images were collected with a Gatan UltraScan® 4000 camera.

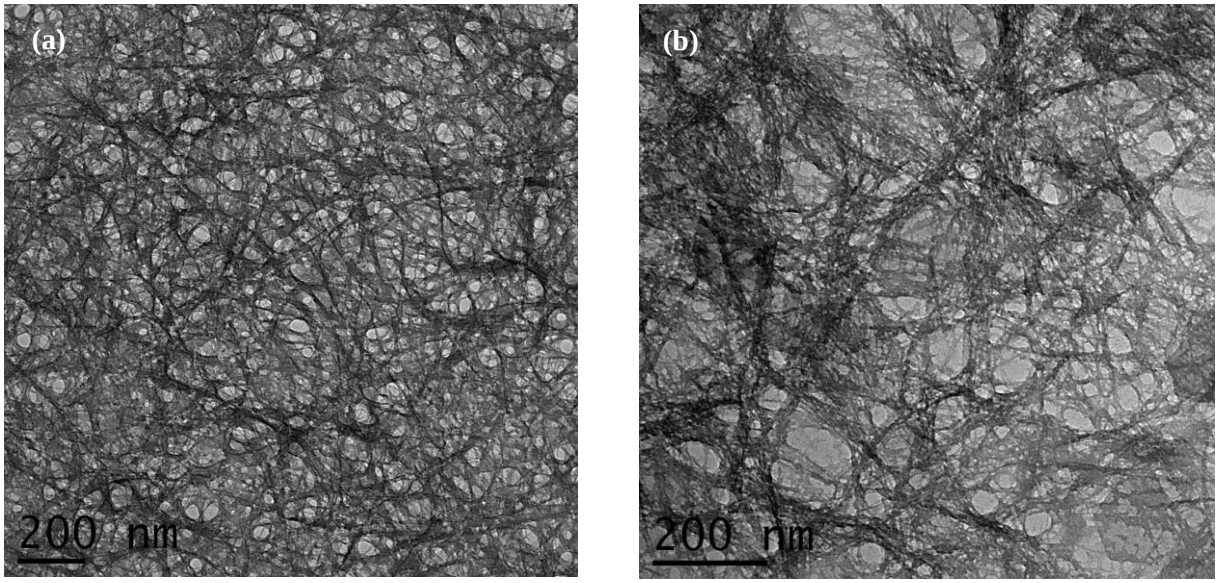

Fig. S4. *TEM images of dried suspensions of imogolite: IMO-OH (a) and IMO-CH_3 (b).*

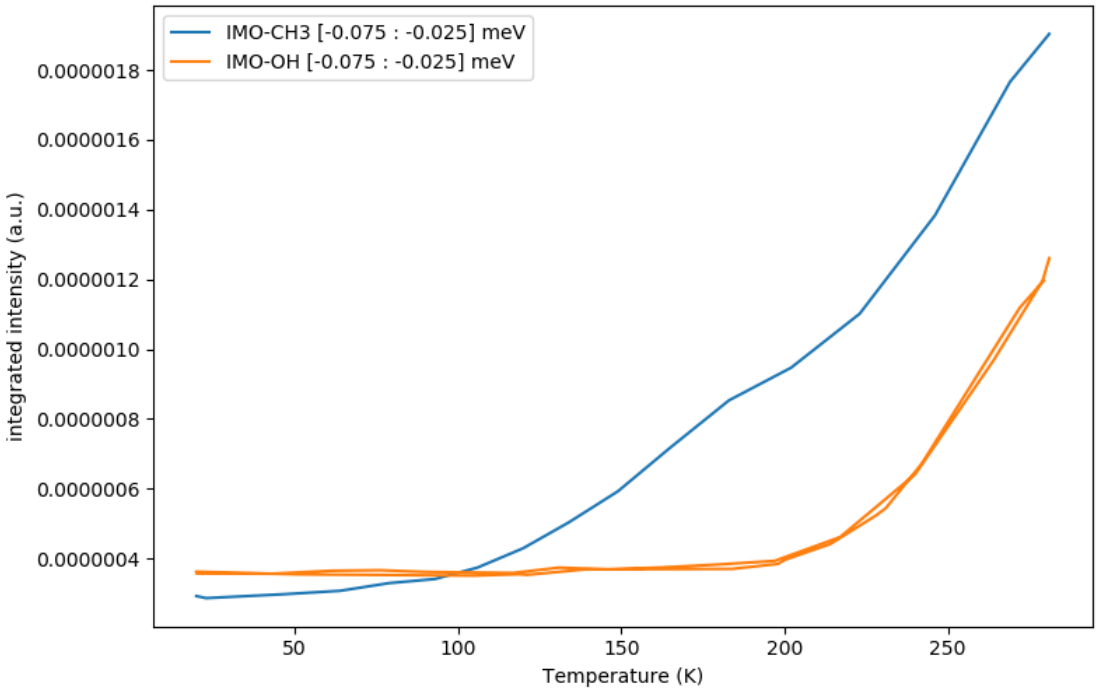

Fig. S5. *Quasi-elastic intensity integrated near the elastic line ([0.025 : 0.075] meV) for IMO-OH and IMO-CH_3 (both 11% RH) versus temperature.*
The integrated energy range selected corresponds to the HWHM of the narrow Lorentzian.
The intensity increases continuously for IMO-CH_3 showing that the dynamics of CH_3 groups activates from very low temperature (around 50 K).
In the case of IMO-OH we observe a very sharp increase of the quasi-elastic intensity from 200 K corresponding to the activation of water and OH groups.

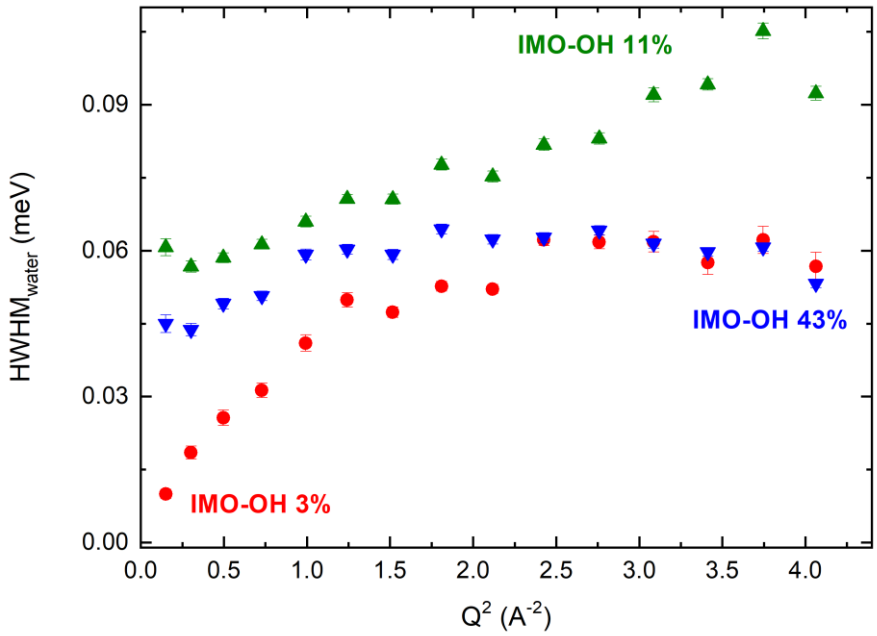

Fig. S6. *HWHM of the narrow Lorentzian component plotted versus Q^2, for the IMO-OH samples equilibrated at 3% (red points); 11% (green up triangles) and 43% RH (blue down triangles) value.*

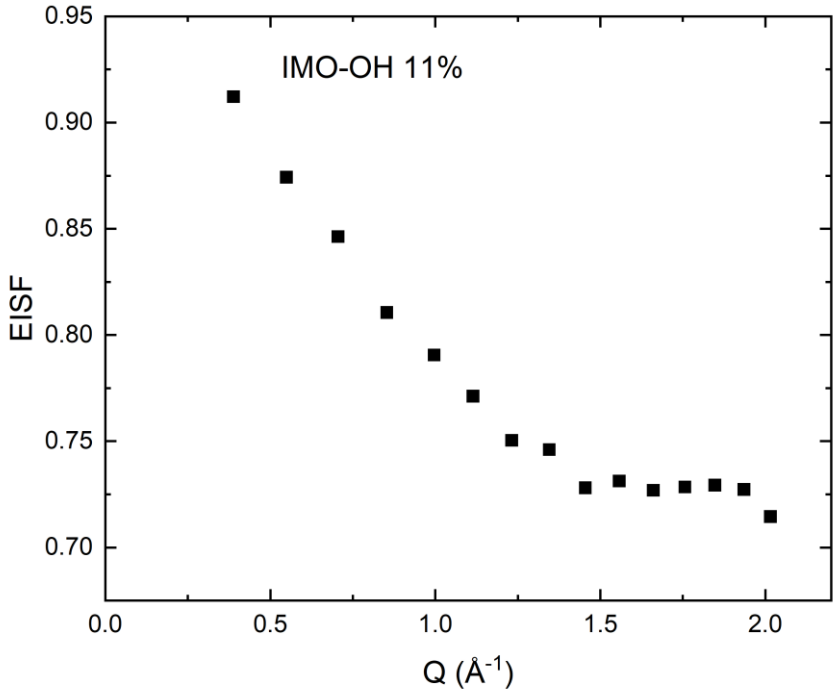

Fig. S7. *EISF data for IMO-OH equilibrated at 11% RH.*

References

(1) Gonzalez, R. I.; Rojas-Nunez, J.; Valencia, F. J.; Munoz, F.; Baltazar, S. E.; Allende, S.; Rogan, J.; Valdivia, J. A.; Kiwi, M.; Ramirez, R. *et al.* Imogolite in Water: Simulating the Effects of Nanotube Curvature on Structure and Dynamics *App. Clay Sci.* **2020**, *191*, 105582.

(2) Konduri, S.; Tong, H. M.; Chempath, S.; Nair, S. Water in Single-Walled Aluminosilicate Nanotubes: Diffusion and Adsorption Properties *J. Phys. Chem. C* **2008**, *112*, 15367-15374.

(3) Scalfi, L.; Fraux, G.; Boutin, A.; Coudert, F.-X. Structure and Dynamics of Water Confined in Imogolite Nanotubes *Langmuir* **2018**, *34*, 6748-6756.

(4) Zang, J.; Chempath, S.; Konduri, S.; Nair, S.; Sholl, D. S. Flexibility of Ordered Surface Hydroxyls Influences the Adsorption of Molecules in Single-Walled Aluminosilicate Nanotubes *J. Phys. Chem. Lett.* **2010**, *1*, 1235-1240.

(5) Or, D.; Tuller, M. Liquid Retention and Interfacial Area in Variably Saturated Porous Media: Upscaling from Single-Pore to Sample-Scale Model *Water Resources Res.* **1999**, *35*, 3591-3605.